# Supplementary Information

# Identifying and controlling phase purity in 2D hybrid perovskite thin films

*Yinghong Hu,[1] Laura M. Spies,[1] Diego Alonso-Álvarez,[2] Priyanka Mocherla,[2] Harry Jones,[3] Jonas Hanisch,[4] Thomas Bein,[1] Piers R. F. Barnes,[2] Pablo Docampo[5,*]*

[1] Department of Chemistry and Center for NanoScience (CeNS), LMU Munich, Butenandtstr. 11, 81377 Munich, Germany

[2] Physics Department, Imperial College London, London, SW7 2AZ, United Kingdom

[3] Physics Department, University of Cambridge, Cambridge, CB3 0HE, United Kingdom

[4] Zentrum für Sonnenenergie- und Wasserstoff-Forschung (ZSW) Baden-Württemberg, Meitnerstr. 1, 70563 Stuttgart, Germany

[5] Physics Department, School of Electrical and Electronic Engineering, Newcastle University, Newcastle upon Tyne, NE1 7RU, United Kingdom

Table S1. Composition of precursor solutions and fabrication parameters for (non)-optimized *n* = 1, 2 and 3 PentA(MA)PI perovskite films.

| | | *n = 1 non-optimized* | *n = 2 non-optimized* | *n = 3 non-optimized* | *n = 2 optimized* | *n = 3 optimized* |
|---|---|---|---|---|---|---|
| precursor solution | $PbI_2$ [mg] | 461.01 | 461.01 | 276.6 | 461.01 | 230.5 |
| | MAI [mg] | 0 | 79.48 | 63.6 | 79.48 | 53.0 |
| | PentAI [mg] | 430.34 | 215.17 | 86.1 | 215.17 | 71.7 |
| | DMF [µL] | 1000 | 1000 | 1000 | 1000 | 1000 |
| | DMSO [µL] | 0 | 0 | 0 | 100 | 350 |
| | THTO [µL] | 0 | 0 | 0 | 100 | 0 |
| spin-coating | speed [rpm] | 3000 | 3000 | 3000 | 3000 | 4000 |
| annealing protocol | | 100 °C, 5 min | 100 °C, 5 min | 100 °C, 5 min | 40 °C, 30 min; 75 °C, 5 min; 100 °C, 2 min | 40 °C, 30 min; 75 °C, 5 min; 100 °C, 2 min |

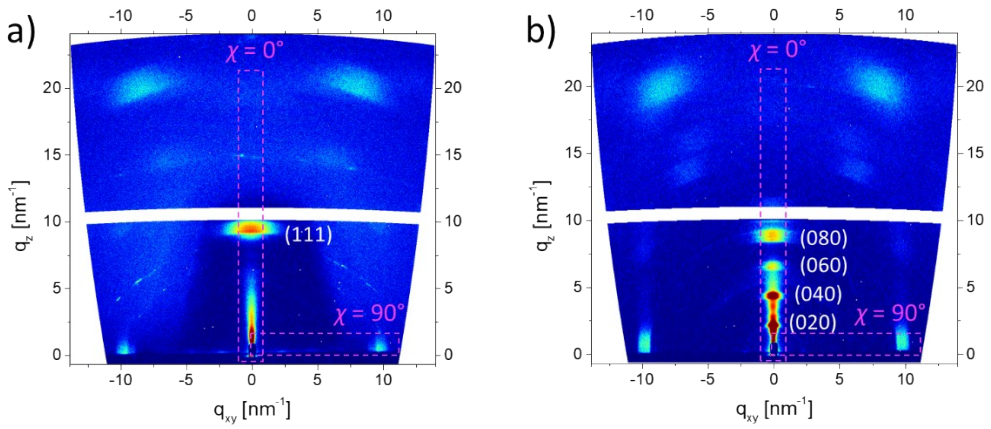


Figure S1. 2D GIWAXS patterns of a) non-optimized and b) optimized $n$ = 3 PentAMAPI films spin-coated on glass. The azimuthal angle $\chi$ is the scattering angle with respect to the $q_z$ axis, with $\chi = 0°$ being the out-of-plane axis and $\chi = 90°$ being the in-plane axis.

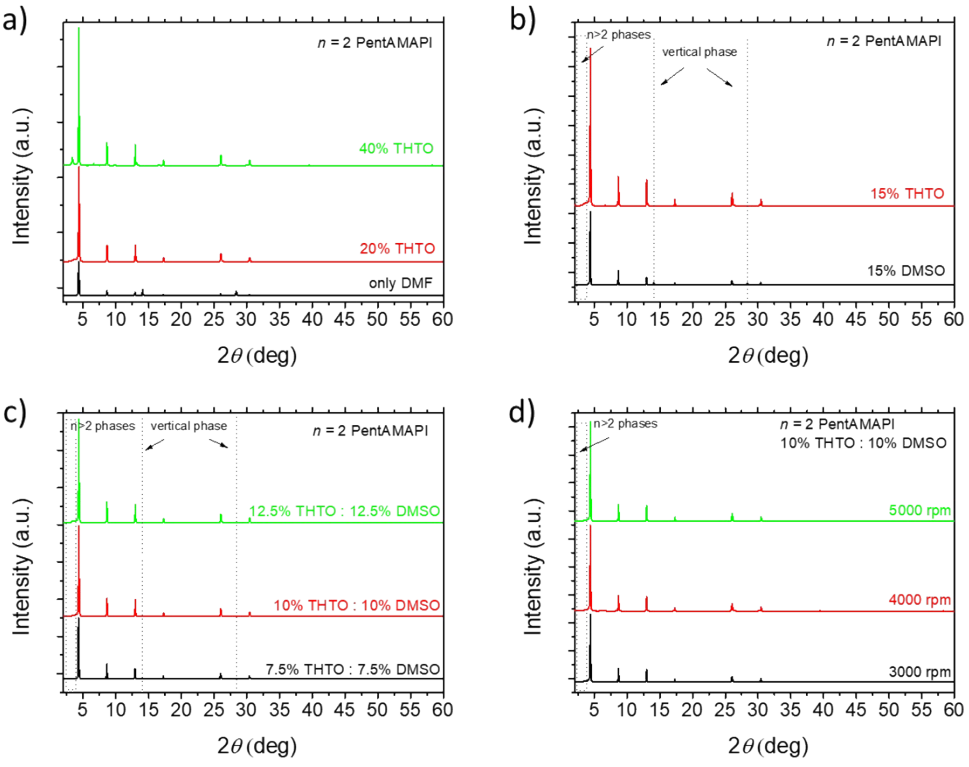


Figure S2. XRD patterns of films on glass substrates spin-coated from $n$ = 2 PentAMAPI solutions with a) different amounts of THTO as solvent additive, b) 15% THTO or DMSO as additive, c) different amounts of THTO and DMSO additives combined and d) using different spinning speeds for the optimized precursor solution.

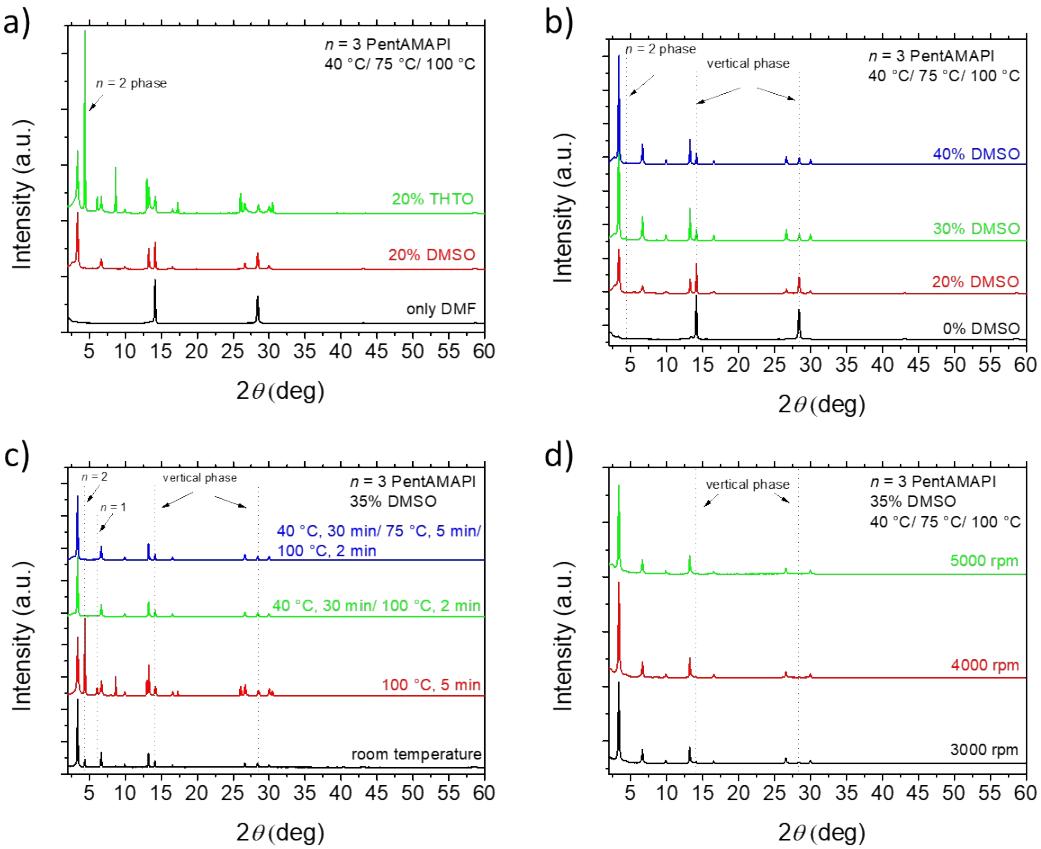


Figure S3. XRD patterns of films on glass substrates spin-coated from $n = 3$ PentAMAPI solutions with a) 20% THTO or DMSO as solvent additive, b) different amounts of DMSO additive, c) varying annealing processes and d) using different spinning speeds for the optimized precursor solution containing ~0.5 M $PbI_2$.

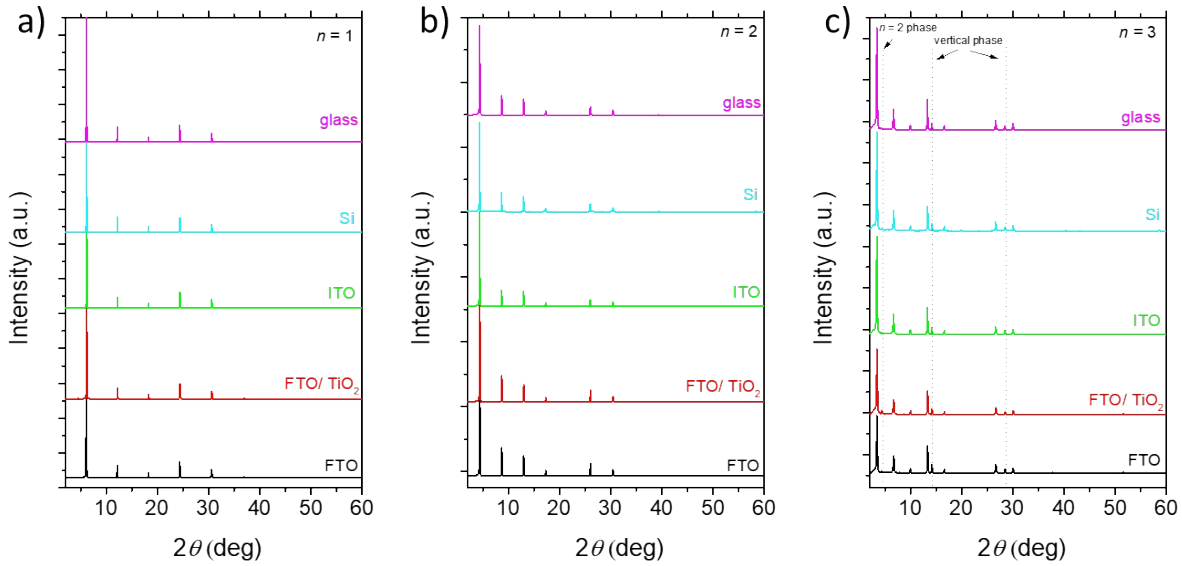


Figure S4. XRD patterns of 2D perovskite films spin-coated on different substrates using a) $n = 1$, b) optimized $n = 2$ and c) optimized $n = 3$ precursor solutions with ~1 M $PbI_2$ concentration and optimized annealing conditions.

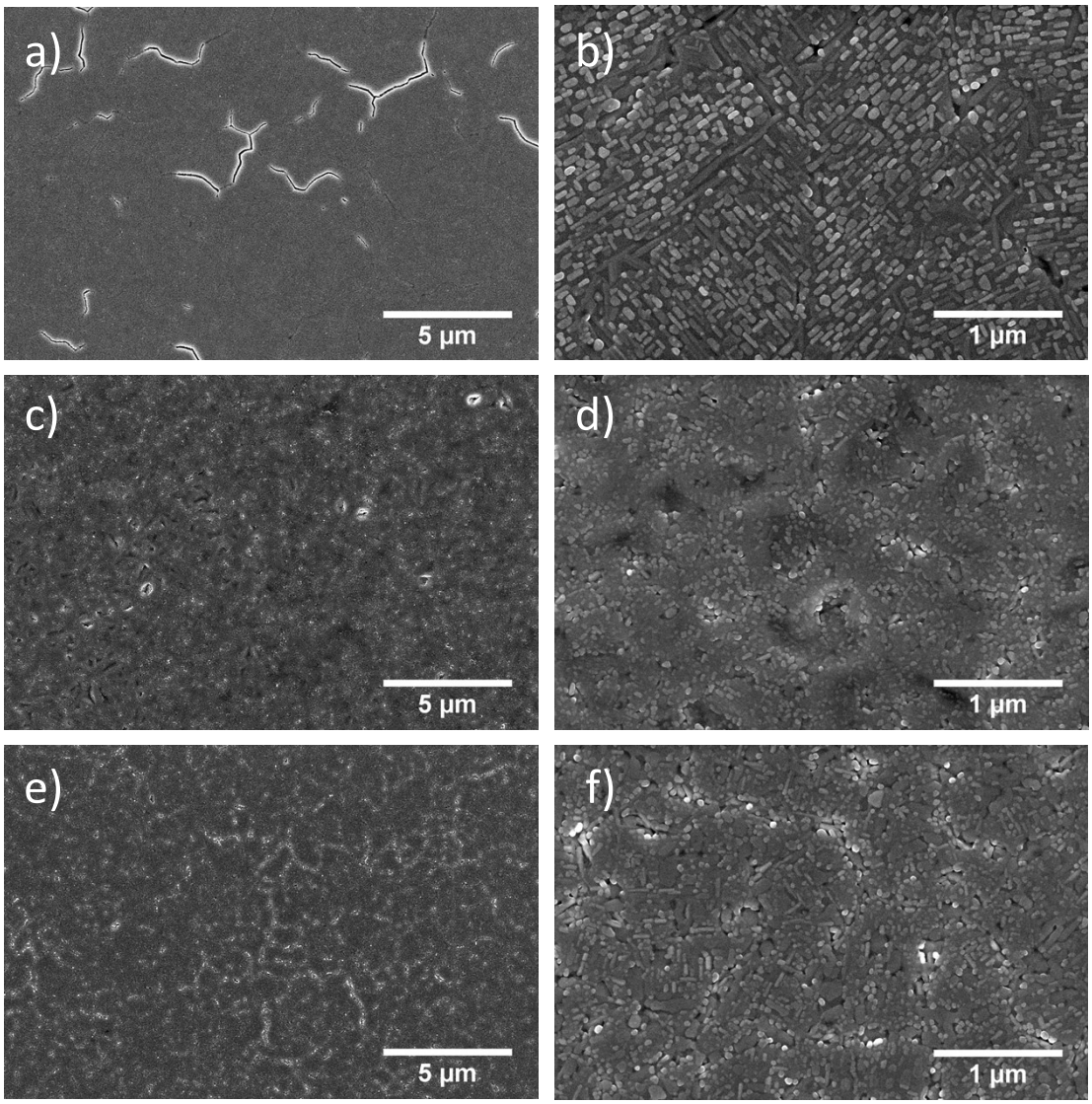


Figure S5. SEM top-view images of 2D perovskite films on FTO/$TiO_2$ substrates with a–b) $n$ = 1, c–d) non-optimized $n$ = 2, and e–f) optimized $n$ = 2.

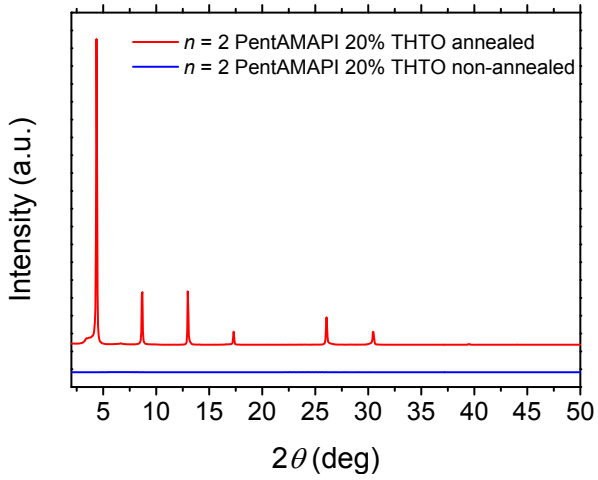


Figure S6. XRD patterns of a film prepared from an $n = 2$ PentAMAPI precursor solution including 20% THTO as solvent-additive, spin-coated on glass substrates before and after annealing (see Table S1 for the optimized annealing protocol).

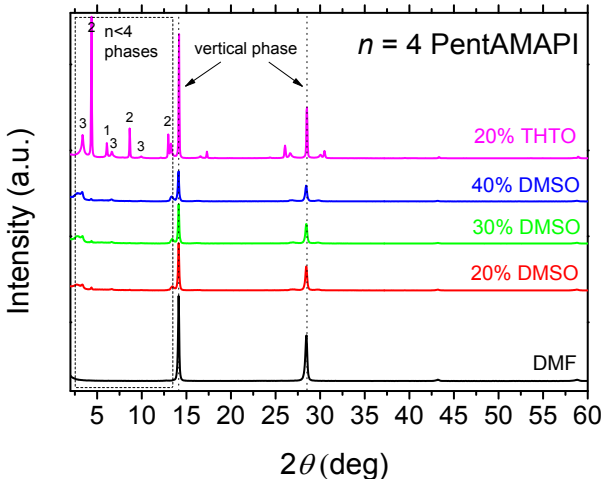


Figure S7. XRD patterns of films prepared from an $n = 4$ PentAMAPI precursor solution (PentAI:MAI:$PbI_2$ = 0.5:0.75:1 mmol in 1 mL DMF) with different amounts of solvent additives and spin-coated on glass substrates. The same annealing protocol as for the optimized $n = 3$ PentAMAPI films was used. The peak labels in the low angle region ($2\theta < 14°$) indicate the $n$-value for the corresponding diffraction peak.